Improved formulas for fusion cross-sections and thermal reactivities

1992 Nucl. Fusion 32 611

(http://iopscience.iop.org/0029-5515/32/4/I07)

IMPROVED FORMULAS FOR FUSION CROSS-SECTIONS AND THERMAL REACTIVITIES

H.-S. BOSCH, G.M. HALE*
Max-Planck-Institut für Plasmaphysik,
Euratom–IPP Association,
Garching/München,
Germany

ABSTRACT. For interpreting fusion rate measurements in present fusion experiments and predicting the fusion performance of future devices or of d–t experiments in present devices, it is important to know the fusion cross-sections as precisely as possible. Usually, it is not measured data that are used, but parametrizations of the cross-section as a function of the ion energy and parametrizations of the Maxwellian reactivity as a function of the ion temperature. Since the publication of the parametrizations now in use, new measurements have been made and evaluations of the measured data have been improved by applying R-matrix theory. The paper shows that the old parametrizations no longer adequately represent the experimental data and presents new parametrizations based on R-matrix calculations for fusion cross-sections and Maxwellian reactivities for the reactions D(d,n)^{3}He, D(d,p)T, T(d,n)^{4}He and ^{3}He(d,p)^{4}He.

1. INTRODUCTION

Fusion cross-sections have been of great interest from the beginning of fusion research, mainly for two reasons: While the detection of fusion reaction products has always been a signature of success, beginning with qualitative measurements of neutron production in the earliest experiments, modern fusion experiments use the measured fusion rates as plasma diagnostics. If one wants to draw reliable conclusions from these measurements about the plasma parameters, detailed knowledge of the fusion cross-sections is more important than ever before. Since the uncertainties in the neutron rate measurements are of the order of 10%, the uncertainties in the cross-sections should be of similar size or slightly lower, i.e. of the order of 5–10%.

As the experimental devices become larger from one generation to the next, it becomes increasingly more important for the design to predict their behaviour reliably. Among other parameters, the fusion rate in these plasmas must be determined accurately. Also, for reactor design and blanket studies, it is necessary to know the energy dependence of the fusion cross-sections with the greatest possible precision, i.e. an uncertainty in the fusion cross-sections of the order of 5% is desirable.

Beginning in the 1940s, there have been many measurements of the fusion cross-sections, mainly for the four most important reactions, D(d,n)^{3}He, D(d,p)T, T(d,n)^{4}He and ^{3}He(d,p)^{4}He. Since these experiments cover only a limited range of energy and are not always in agreement, the data have been periodically collected and reviewed, usually resulting in some graphical or, more recently, analytical representation of the cross-sections. Today, such parametrizations of the data are essential, since the use of tables is not so convenient.

Two approximate representations of the fusion cross-sections have been widely used, one derived by Duane in 1972 [1], which is also listed in the NRL formulary [2], and the other derived by Peres in 1979 [3]. Duane's cross-sections pose particular difficulties if they are extrapolated to energies below about 20 keV because of the unphysical parametrization of the penetrabilities that was used. In general, however, both approximations as well as the corresponding parametrizations for the Maxwellian reactivity $\langle \sigma v \rangle$ calculated by Hively [4, 5] (on the basis of Duane's cross-section formula) and by Peres [3] are no longer adequate, for two reasons: First, in the last few years there have been new and more accurate measurements of the fusion cross-sections which in any case justify new parametrizations. Second, the development since the 1970s of multi-reaction, many-observable R-matrix analyses for systems containing the major fusion reactions has provided a much better method of evaluating the cross-section data.

In this paper, we make use of cross-section information based on more recent experiments and on the more reliable representations given by R-matrix theory [6] to

* Permanent address: Theoretical Division, Los Alamos National Laboratory, Los Alamos, NM 87545, USA.

derive better parametrizations for fusion cross-sections and Maxwellian reactivities. The paper is divided into three parts. After a short introduction into the physics of the fusion reactions and R-matrix theory, we compare the data now available with the old parametrizations (to give an idea of their validity and accuracy), and also with the cross-section values resulting from R-matrix calculations. In the third part, we derive new parametrizations based on these R-matrix data for the fusion cross-sections as well as for the reactivities in thermal plasmas.

2. THEORETICAL BACKGROUND

The physics of fusion reactions between light nuclei has been treated in detail elsewhere [7, 8], and detailed information on the states of the intermediate compound systems has been collected in two review papers [9, 10]. Here, we only discuss some basic physics issues that are necessary to understand the parametrization used.

2.1. Parametrization of the cross-section

Fusion reactions between two nuclei can be divided into two parts which are approximately independent of each other, namely the atomic physics of the nuclei approaching each other, and the nuclear physics valid if they are close enough to feel the nuclear forces. The strong energy dependence of the fusion cross-section (see Fig. 1(a)) is mainly due to the repulsive Coulomb potential. As long as the energy available in the centre-of-mass (CM) frame is much smaller than the Coulomb barrier, reactions are possible only because of the tunnelling effect, and the cross-section is proportional to the tunnelling probability:

$$\sigma \sim \exp - \frac{2\pi Z_1 Z_2 e^2}{\hbar v} \qquad (1)$$

with v being the relative velocity of the reacting particles [11]. This can be rearranged to give

$$\sigma \sim \exp (-B_G/\sqrt{E}) \qquad (2)$$

where

$$B_G = \pi \alpha Z_1 Z_2 \sqrt{2 m_r c^2} \qquad (3)$$

is the Gamov constant, expressed in terms of the fine structure constant, $\alpha = e^2/\hbar c = 1/137.03604$, and the reduced mass of the particles, $m_r c^2$, in keV. Throughout this paper, E denotes the energy available in the CM frame. For a particle A with mass m_A striking a stationary particle B, the simple relation $E_A = E\,(m_A + m_B)/m_B$ holds.

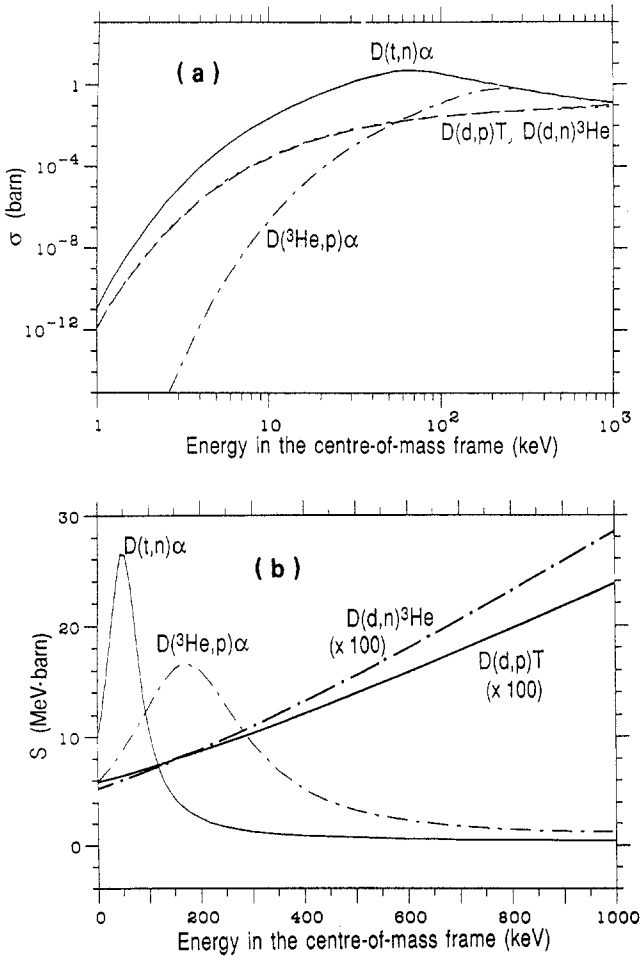

FIG. 1. (a) Fusion cross-sections for the most important fusion reactions as a function of the CM energy of the reacting particles. The curves are calculated from Peres' [3] formula. (b) The S-functions for these reactions as derived from Eq. (4). For the d + d reactions the data have been multiplied by 100 to improve clarity.

Quantum mechanics shows that the fusion reaction probability is also proportional to a geometrical factor $\pi\lambda^2 \sim 1/E$, where λ is the de Broglie wavelength. The strong energy dependences of this factor and the barrier penetrability have prompted the introduction of the astrophysical S-function [12, 13], defined by writing the cross-section as a product of three factors:

$$\sigma = S(E) \frac{1}{E} \exp (-B_G/\sqrt{E}) \qquad (4)$$

The motivation for this definition is that the two well known, strongly energy dependent factors (which describe the Coulombic and phase space parts of the incident channel) are separated, leaving the S-function to represent mainly the presumably slowly varying nuclear part of the fusion reaction probability [13].

The S-functions for the four reactions shown in Fig. 1(b) demonstrate very clearly the advantages of using the S-functions instead of the cross-sections:

— The S-function describes mainly the intrinsic nuclear physics of the reaction and therefore shows clearly the difference between the reactions considered here. The d + d reactions do not have strong S-wave resonances close to the threshold, resulting in a weak energy dependence, while the other two reactions involve a near-threshold S-wave resonance of the compound system. This is very evident in the S-function, while in the cross-section it is masked by the strong energy dependence of the Coulomb barrier penetration.
— In all cases, the S-functions only vary by a factor of 20 over the energy range shown here, instead of by about 14 orders of magnitude. Therefore, it is much easier to not only compare data on a linear scale over a wide range but also to calculate a reasonable fit to the data.

While the first point is more important for nuclear physicists, the second one has practical significance when displaying and comparing the cross-section data, and obtaining parametric representations of the R-matrix calculations.

Strictly speaking, the factorization of the cross-section given by Eq. (4) holds only at energies for which the nuclear reaction is dominated by incident S-wave transitions. Furthermore, the Gamov penetrability form used there is appropriate only as long as the energy of the particles is much smaller than the barrier potential [7]. (The Coulomb barrier is $\approx$210 keV for the d + d reactions, $\approx$280 keV for d + t and $\approx$580 keV for d + ^{3}He, calculated using the channel radii from the R-matrix calculations.) Some authors [1, 3] have tried to extend the validity of the factorized cross-section expression to higher energies by using the somewhat more general penetrability function of Mott [14] giving

$$\sigma = \frac{S^*(E)}{E\,[\exp(B_G/\sqrt{E}) - 1]} \qquad (5)$$

At the energies where the two tunnelling probabilities differ, however, neither of them gives a particularly good representation of the true Coulomb barrier penetrability, and, since we regard the factorization simply as a mathematical normalization, it does not matter which form is used. Bearing in mind the possibility of integrating the cross-section analytically, as is sometimes done in reactivity calculations [15, 16], we use the definition from Eq. (4) since only this simpler form can be integrated analytically.

A factorized form such as Eq. (4) or (5) can always be used at higher energies, of course. It simply means that the S-function thus defined must increasingly include the barrier penetration effects of Coulomb repulsion and higher angular momenta [17] that are not contained in the simple Gamov or Mott penetrabilities. In this way, we have found it possible to use Eq. (4) to parametrize the calculated cross-sections at energies of up to 5 MeV without putting too severe a strain on the energy dependence of the S-function.

2.2. The old cross-section parametrizations

Duane [1] used for his parametrization Mott's form of the Coulomb barrier penetrability as given in Eq. (5) and approximated the S-function as the sum of a constant and a single-level Breit–Wigner resonance term:

$$\sigma = \left[\frac{A_2}{1 + (A_3 \cdot E_d - A_4)^2} + A_5\right] \times \frac{1}{E_d\,[\exp(A_1/\sqrt{E_d}) - 1]} \qquad (6)$$

The energy variable in this formula is the laboratory energy E_d of the deuteron. The main problem with the parametrization of Duane, however, is that he also considered the constant in the exponent (A_1 in his formula) in the tunnelling probability as a free parameter that could be varied to fit the data. The A_1 values resulting from the fits differ significantly (even small differences in an exponent are significant) from the expected values given in the CM system by Eq. (3), and they are different for the D(d,n)^{3}He and D(d,p)T reactions even though the incident channel is the same in both cases. While these unphysical parameter values accounted reasonably well for the cross-section data in the limited energy ranges of the fits, they give poor extrapolations of the cross-sections to low energies, being in severe disagreement with more recent measurements, especially those for the branching ratio of the d + d reactions, as we shall see in Section 6.

Peres [3] used the factorization according to Eq. (5) to derive S*-values from the experimental data. He then fitted these values with a polynomial in a Padé expansion:

$$S^* = \frac{A1 + E(A2 + E(A3 + E(A4 + EA5)))}{1 + E(B1 + E(B2 + E(B3 + EB4)))} \qquad (7)$$

Here, again, E is the energy available in the CM frame. This parametrization shows no systematic deviations from the data and has proved to be a very flexible fit formula. Sadler and Van Belle [18] therefore used the

same procedure as Peres to fit the new $T(d,n)^4He$ measurements from Los Alamos [19].

As discussed above, we will use the penetrability form of Eq. (4), but with a Padé polynomial expansion of the S-function, to represent cross-sections resulting from R-matrix analyses of the type described in the following section.

2.3. R-matrix theory

R-matrix theory [20, 21] provides a mathematical description (and a simple parametrization) of nuclear reactions that is relatively model independent. It presumes that, owing to the short range of nuclear forces, there exist 'channel radii' outside of which a many-body nuclear system exhibits only two-body degrees of freedom. By putting the known two-body wave functions in these regions explicitly into the theory, it incorporates the Coulomb and angular momentum barrier penetration effects exactly at all energies, overcoming the shortcomings of cross-section parametrizations based on Eqs (4) or (5).

Being a multi-channel theory, R-matrix theory describes different reactions in the same compound system (as in the ^4He system reactions $T(p,p)T$, $D(d,n)^3He$, $D(d,p)T$, etc.) simultaneously with a single set of parameters. All types of experimental data (integrated cross-sections, differential cross-sections, polarizations, etc.) for all reactions therefore can be used to determine the R-matrix parameters of the system. The constraints imposed by using a very large dataset and a physically meaningful theoretical framework for the parametrization result in a better determination of any particular cross-section (in our case the integrated fusion) than can be obtained from direct measurements of that cross-section alone.

The multi-reaction, many-observable approach to doing R-matrix analyses was pioneered by Dodder and Hale at Los Alamos in the 1970s. Their analyses of the light systems containing fusion reactions [6] have resulted in R-matrix parameters that clarify the level structure of these systems [22, 23] and give fusion cross-section predictions that, despite being in some cases more than ten years old, still give good representations of even the most recent experimental data. The cross-sections calculated from those analyses [24, 25] therefore form the basis of our new parametrizations of the fusion cross-sections and reactivities. Since the calculation of cross-sections from multi-level R-matrix parameters is not trivial, however, we have used the representation given by Eq. (4) to derive more convenient numerical fits to the R-matrix calculations, which are presented in Section 4.

3. REVIEW OF THE EXPERIMENTAL DATA

In this section we compare a selection of the available experimental cross-section data with the well known parametrizations and with the Los Alamos R-matrix calculations. The emphasis here is on the data measured after the parametrizations calculated by Duane and Peres. A more complete overview of the experimental data has been given in Ref. [17].

3.1. Data for the reaction $T(d,n)^4He$

The experimental data on this reaction are shown in Figs 2–4. Most of these data were taken for energies (in the CM frame) below 500 keV, with special emphasis on the resonance at E = 64 keV (or E_d = 107 keV). The separation of the tunnelling probability, however, shifts the maximum, which occurs at E ~ 48 keV for the S-function, as can be seen in these plots.

Duane used for his fit [1] the data published by Brolley et al. [26], Argo et al. [27], Conner et al. [28], Stratton and Freier [29], Arnold et al. [30], Hemmendinger and Argo [31], and Bame and Perry [32]. From Arnold's experiments the original data [33] are shown in Fig. 2, not the data from a smoothed curve which were published later [30] and which are normally used. Peres [3] used all the data published in

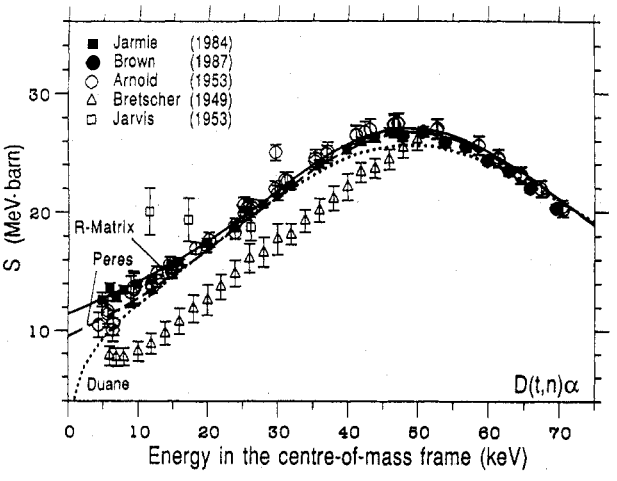

FIG. 2. S-values as a function of the energy available in the CM frame for the d + t reaction. The S-values were derived from the experimental data mentioned in the figure. Bretscher's data [44] are much too low and do not show the maximum, while Jarvis' data [34] do not even follow the trend of the data. The new Los Alamos data confirm quite well the measurements of Arnold et al. [33], except at the very low energies, where Arnold's data are too low.

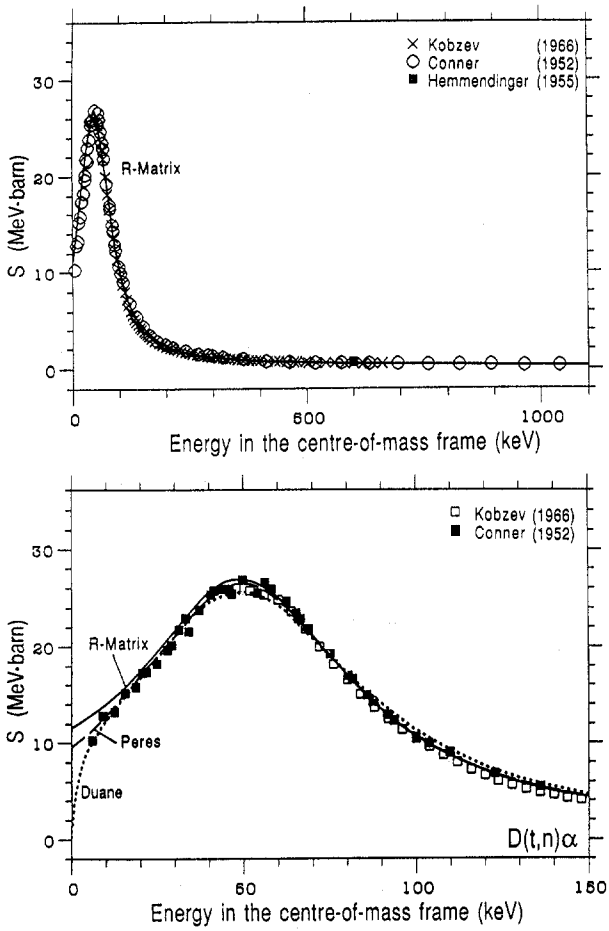

FIG. 3. S-values as derived from the measurements of Katsaurov [41] in 1962 (also published by Kobzev et al. [40] in 1966) and from Conner et al. [28] in 1952. The error bars given by these authors are smaller than the symbol size in this figure and they have therefore been omitted. Data have been published for energies up to 1 MeV, but this figure has been restricted in order to show the region of the resonance in greater detail. These data agree very well with the parametrizations of Duane and of Peres, and they are a little lower than the R-matrix evaluation.

Refs [27, 30, 32] as well as those by Jarvis and Roaf [34] and by Smith and Thornton [35], and Conner's data for E ≤ 450 keV only.

For this reaction, Liskien and Paulsen [36] calculated a spline fit to the data which was published as a table of cross-section data. In this calculation the cross-section data were taken from Refs [27, 28, 30–32 and 37–40]. However, in Ref. [40], only the measurements taken by Katsaurov in 1962 [41] are reproduced.

Figure 2 also shows the most recent measurements from the group at Los Alamos [19, 42, 43]. The data taken by Bretscher and French in 1949 [44] and by Jarvis and Roaf in 1953 [34] do not follow the trend of all the other data and should not be used for any parametrization.

At energies around the maximum, the parametrization of Duane [1] is about 5% lower than most of the experimental data, while Peres' formula [3] and the R-matrix calculation follows them closely. At very low energies, the Duane parametrization decreases sharply, following the data of Conner et al. [28] (see Fig. 3) and Arnold et al. [33]. The error bars of Arnold's data, however, also would fit Peres' parametrization, which is much flatter at these energies. The data from Jarmie et al. [19] and Brown et al. [43] are higher and also indicate a flat S-function, a trend also shown by the R-matrix theory. This means that the Duane parametrization has its greatest error at the very low energies, as expected from the discussion of the previous section.

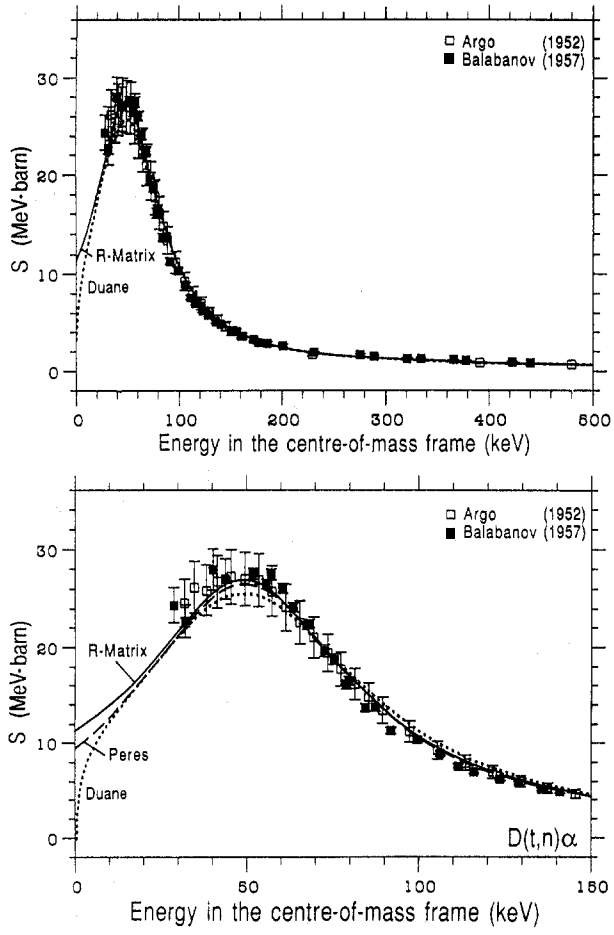

FIG. 4. S-values as derived from the measurements of Argo et al. [27] in 1952 and from Balabanov et al. [38] in 1957. The error bars are quite large in the region of the resonance, but the data are even above the values from the R-matrix calculation. Again, this figure shows only a part of the data which have been measured up to 500 keV.

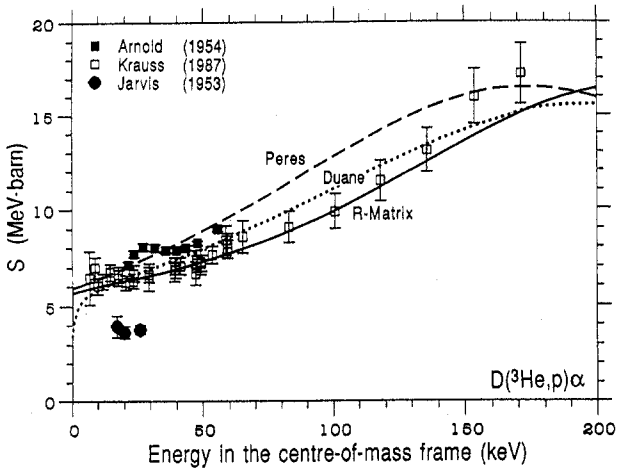

FIG. 5. S-values as a function of the energy available in the CM frame for the d + ^{3}He reaction. Jarvis' data [34] are much too low and should not be used for any evaluation. Krauss' data [50] were measured long after the R-matrix had been calculated, but they agree rather well with it, except for the two points at the highest energies.

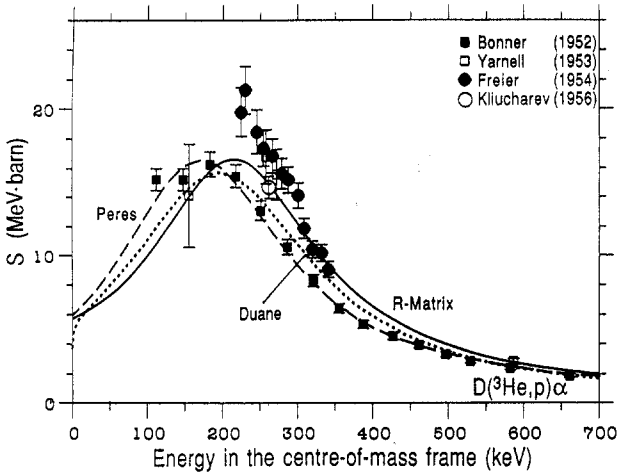

FIG. 6. S-values as a function of the energy available in the CM frame for the d + ^{3}He reaction. It was mainly the dataset of Bonner [45] that determined Peres' fit, as can be seen here.

3.2. Data for the reaction ^{3}He(d,p)^{4}He

All the experimental data on this reaction are shown in Figs 5–7. The most recent data collection on the nuclear physics of the ^{5}Li compound nucleus involved in this reaction shows that the resonance should occur at E = 270 keV (or E_d = 450 keV). The experimental data for this reaction, however, show large discrepancies with respect to the absolute cross-section values and the position of the resonance, as can be seen in these figures. The measurements of Arnold et al. [30] covered only the very low energy region far below the resonance. Again (as in Fig. 2) the data of Jarvis and Roaf [34] are completely off. The data of Bonner et al. [45] and the measurements of Kunz [46] showed a resonance with a rather low maximum (and in different positions), while the data of Yarnell et al. [47] and of Freier and Holmgren [48] showed much higher values. They could not, however, reveal the position of the maximum of the S-function.

The new measurements of Möller and Besenbacher [49] and of Krauss et al. [50] show a maximum at an energy close to that of Kunz [46], and their absolute values are between those of Bonner et al. [45] and Kunz [46] and those of Arnold et al. [30], Yarnell et al. [47] and Freier and Holmgren [48].

Duane [1] used for his fit the data published in Refs [30, 34, 45–48 and 51]. Allred [51], however, took experimental data only for an energy of about 5 MeV and this point is not shown here.

Peres [3] used only the data from Arnold et al. [30] and Bonner et al. [45], as can be very clearly seen in Figs 5 and 6. He explicitly rejected the data of Jarvis and Roaf [34].

Because of discrepancies in the experimental data taken before 1979, these parametrizations look very different, and it is not clear how to solve this problem. The more recent data of Möller and Besenbacher [49] and of Krauss et al. [50] are between the two groups of data mentioned before, but they do not allow a decision to be made on the old data.

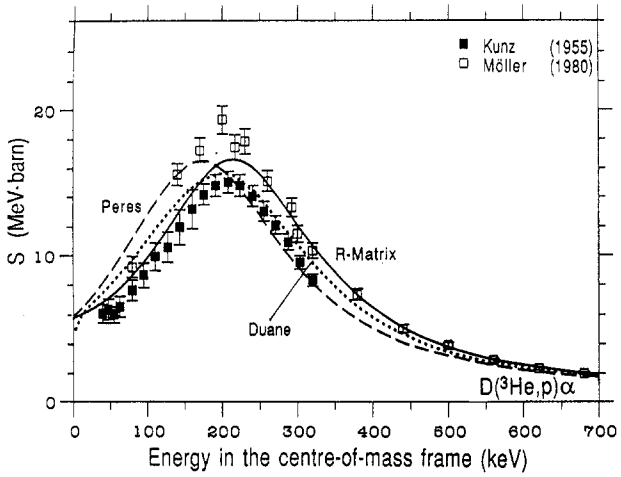

FIG. 7. S-values as a function of the energy available in the CM frame for the d + ^{3}He reaction. The data of Möller et al. [49] were taken after the R-matrix calculation, but they agree rather well with these results, except in the region just below the resonance.

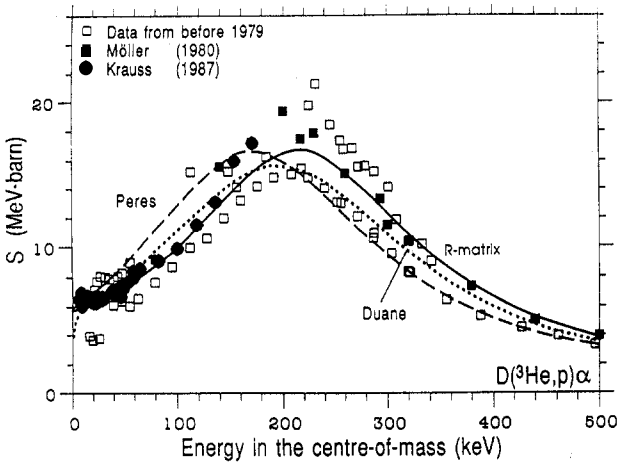

FIG. 8. S-values as a function of the energy available in the CM frame for the $d + {}^3He$ reaction. The light squares mark all the data taken before 1960, and the solid line shows the results of the R-matrix calculation from 1979, based on these data and on data for other reactions. The dark symbols show the data taken later, which agree rather well with these R-matrix results, except for some discrepancy in the region of the resonance.

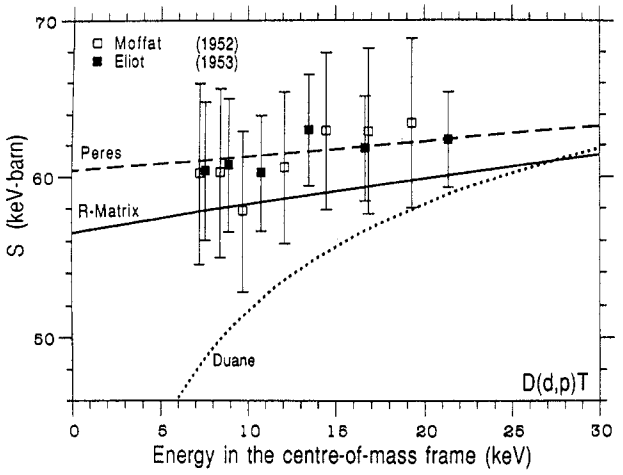

FIG. 9. S-values as a function of the energy available in the CM frame for the D(d,p)T reaction. Although both datasets have appreciable error bars assigned to them, they clearly disagree with the trend of Duane's parametrization.

The solution to this problem, however, comes from the R-matrix fit, as can be seen in Fig. 8. The light squares mark the data from before 1960, and the solid line shows the cross-sections calculated from the R-matrix fit in 1979. The error bars have been omitted for clarity, but the R-matrix calculation does not appear to give a good fit to these data. Obviously, it is mostly the experimental data from other reactions and the physical constraints of the model that have determined the calculated integrated cross-sections. The measurements of Möller and Besenbacher [49] and of Krauss et al. [50], made after the analysis was done, agree very well with the R-matrix result except just around the resonance. This illustrates impressively our point that R-matrix methods really improve cross-section evaluations (even if the experimental cross-section data are in mutual disagreement) by also including other types of measurements and data from other reactions.

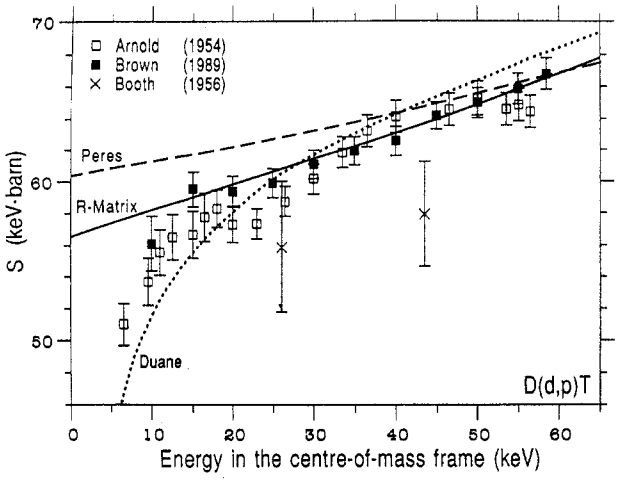

FIG. 10. S-function of the D(d,p)T reaction. Arnold's data [30] (points of a smooth curve through the experimental data) decrease sharply towards low energies, unlike all other datasets. The data of Booth et al. [62] are much lower than all the other data and should not be used for a parametrization.

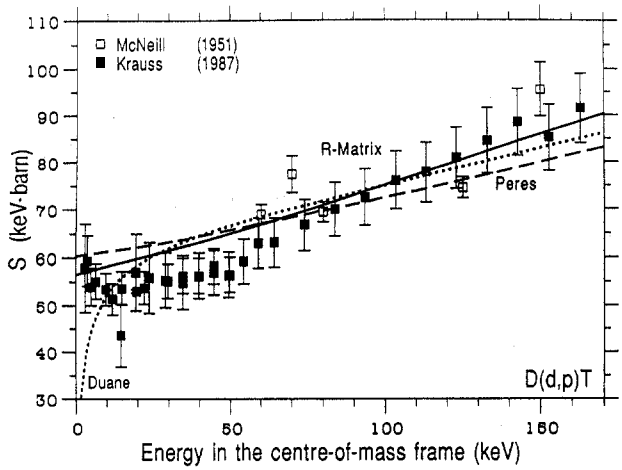

FIG. 11. S-function of the D(d,p)T reaction. Krauss et al. [50] used two different accelerators for their measurements, and the very low data point at about 15 keV is the lowest energy point of the high energy accelerator experiments.

3.3. Data for the reaction D(d,p)T

Although the fusion reactions D(d,p)T and D(d,n)^{3}He have no obvious resonance behaviour at low energies, they show an anisotropic emission of the fusion reaction products in the CM frame, unlike the resonant reactions considered before. Many measurements of this anisotropy have been performed, and they have been summarized by Theus et al. [52]. More recent measurements can be found in Refs [50, 53, 54], but here we want to discuss only the total cross-section data.

For the D(d,p)T reaction, the S-functions calculated from a selection of the experimental data are shown in Figs 9–12. Duane [1] calculated his fit from the data published by Arnold et al. [30], Blair et al. [55], Moffat et al. [56], Davenport et al. [57], Eliot et al. [58] and Preston et al. [59]. Peres' approximation formula [3] was calculated from the data of Arnold et al. [30], Moffat et al. [56], Davenport et al. [57], Preston et al. [59], MacNeill and Keyser [60], Wenzel and Whaling [61], Booth et al. [62], Brolley et al. [63], and Schulte et al. [64]. However, Schulte published Legendre coefficients only, and his data are not shown in this paper. Since the data of Blair et al. [55] and of Brolley et al. [63] cover the energy region above 500 keV (up to 7 MeV), they are also not shown here (see Ref. [17]). In addition to the data mentioned before, we show the recent data of Krauss et al. [50], Brown and Jarmie [54] and Jarmie and Brown [65].

The data of Booth et al. [62] are far below all the other data and should not be used for any parametrization. Again, we see that Duane's parametrization decreases sharply towards low energies (where it is normally used), and the only dataset following this trend is the one of Arnold et al. [30]. However, the data published by Arnold in 1954 are not the originally measured data, but points from a smooth curve through his experimental data. All the other data at energies below about 15 keV are rather flat and agree with Peres' parametrization and the R-matrix results, thereby indicating that the Duane parametrization is seriously in error at these low energies. In the energy range 150–600 keV, all data are much higher than both of the old parametrizations, but they agree very well with the R-matrix result.

3.4. Data for the reaction D(d,n)^{3}He

The experimental data on this reaction are shown in Figs 13–15. Duane used for his fit [1] the data published by Arnold et al. [30], Blair et al. [55]*, Preston et al. [59], Erickson et al. [66], Hunter and Richards [67]*, and unpublished data by Smith et al. Peres' approximation formula [3] was calculated from the data of McNeill and Keyser [60], Arnold et al. [30], Booth et al. [62], Brolley et al. [63]* and Schulte et al. [64]*. Peres explicitly rejected the data of Preston. All the data denoted with * have been taken at energies between about 500 keV and 7000 keV, and they are not shown here (see Ref. [17]).

For this reaction, tables with differential cross-section data and total cross-section data have been published [36, 68]. Liskien and Paulsen [36] used the data of Blair

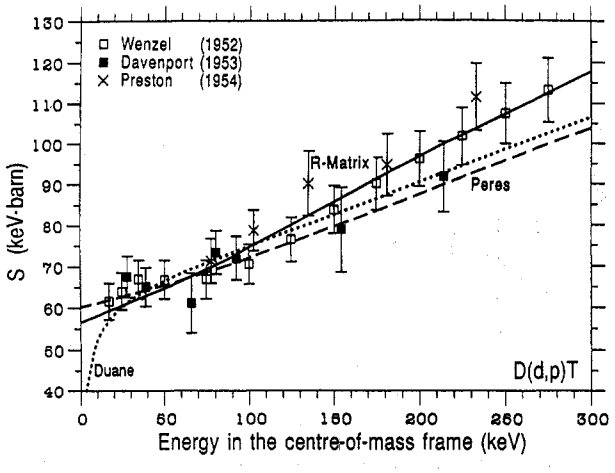

FIG. 12. S-function of the D(d,p)T reaction. The data of Wenzel and Whaling [61] and those of Preston et al. [59] are much higher than the old parametrizations for energies above about 200 keV.

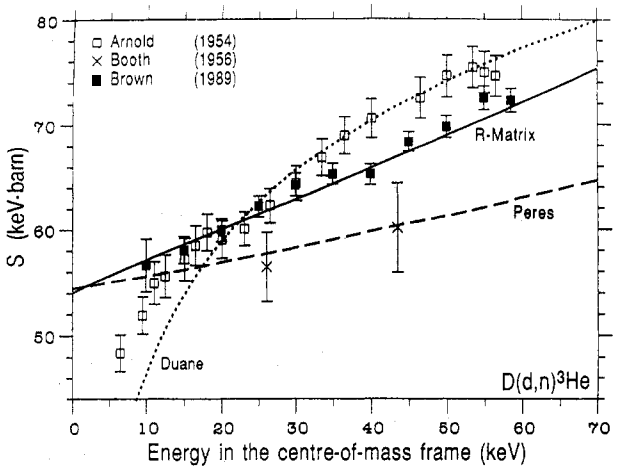

FIG. 13. S-function of the D(d,n)^{3}He reaction. As in the case of the D(d,p)T reaction, Arnold's data [30] decrease sharply towards low energies, unlike all other datasets, and again the data of Booth et al. [62] are too low. Arnold's data have been corrected as described in the text.

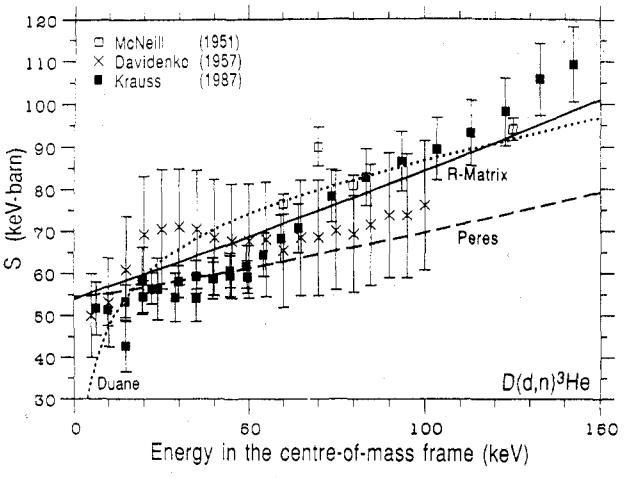

FIG. 14. S-function of the D(d,n)^{3}He reaction. The data of McNeill and Keyser [60] have been corrected as described in the text.

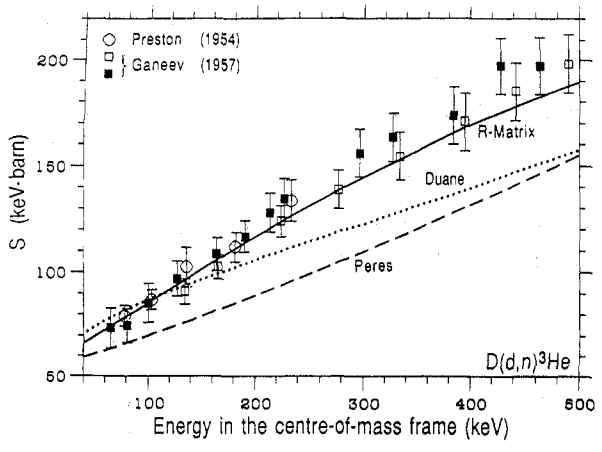

FIG. 15. S-function of the D(d,n)^{3}He reaction for higher energies. Ganeev et al. [69] used two different methods — numerical integration of differential cross-sections (light squares) and measurements in a $KMnO_4$ bath (black squares). Again, in this energy region all experimental data are higher than the old parametrizations and agree with the R-matrix results.

et al. [55]*, McNeill and Keyser [60], Hunter and Richards [67]*, Arnold et al. [30], Preston et al. [59], Booth et al. [62], Brolley et al. [63]*, Ganeev et al. [69], Davidenko et al. [70], Goldberg and Le Blanc [71]*, Thornton [72]* and Schulte et al. [64].

The data of Arnold et al. [30] are again points of the smooth curve through the experimental data, and these data also agree with Duane's parametrization, unlike all the other datasets. There was, however, a problem with the D(d,n)^{3}He data of Arnold and McNeill. Both of them measured the differential cross-section for one angle only and then used the angular distribution of the D(d,p)T reaction to calculate absolute cross-sections (believing that the angular distributions for both the d + d reactions are equal, which is not the case). Later, McNeill found this problem and published corrected data [73]. It is not clear which datasets Duane, Peres and Liskien used, but in this paper the corrected data are shown. Ganeev et al. [69] used two different methods: they measured $d\sigma/d\Omega$ for a few angles and integrated this curve (light squares in Fig. 15), and they made measurements in a $KMnO_4$ bath, thereby measuring the total neutron yield directly (black squares in Fig. 15).

At energies below about 50 keV, there is a wide spread in the experimental data, and this is reflected in the old parametrizations. The new data of Krauss et al. [50] and of Brown et al. [43] do not follow either of these parametrizations, but they agree well with the R-matrix results. This is also true for the energy range 150–600 keV, where all the data are much higher than both of the old parametrizations.

4. CROSS-SECTION PARAMETRIZATION

As discussed in Section 3, the cross-section parametrizations now in use do not adequately represent the recent experimental data, and they differ strongly from R-matrix calculations of the cross-sections that are based on many kinds of experimental data.

The multichannel R-matrix parametrizations discussed here generally involve fewer than 100 parameters from which the cross-section can be calculated. This calculation, however, is rather lengthy and inconvenient. Therefore, we have used the calculated cross-sections to derive a more convenient and compact representation of the R-matrix results for use over a limited energy range.

4.1. Cross-sections from R-matrix analyses

The R-matrix analysis of the ^{5}He system is complete and has been published [22] in part. The T(d,n)^{4}He cross-sections from that analysis are determined to within 2% at energies of up to 1 MeV, with the error gradually increasing up to about 5% at higher energies. Table I shows some details of this analysis and demonstrates clearly that the additional input of data other than the total fusion cross-sections increases the database significantly.

The R-matrix calculations for the d + ^{3}He reaction date back to July 1979. However, the data taken later agree with this evaluation, which is supposed to be correct to at least 10% (with the maximum uncertainty

TABLE I. SUMMARY OF THE ^{5}He SYSTEM R-MATRIX ANALYSIS[a]

Channel	ℓ_{max}	a_c (fm)
d-t	3	5.1
n-^{4}He	4	3.0
n-^{4}He[a](0^+)	1	5.0

Reaction	Energy range	Number of observable types	Number of data points	χ^2
T(d,d)T	E_d = 0-8 MeV	6	695	1147
T(d,n)^{4}He	E_d = 0-8 MeV	14	1020	1423
T(d,n)^{4}He[a](0^+)	E_d = 4.8-8 MeV	1	10	17
^{4}He(n,n)^{4}He	E_n = 0-28 MeV	2	795	1160
	Totals	23	2520	3767

[a] The top part gives the maximum angular momentum quantum numbers and the channel radii used for the different channels in this system, while the bottom part summarizes the data included for each reaction, and some details of the fit, for which the overall χ^2 per degree of freedom is 1.55.

occurring near the peak of the resonance), and therefore we will use the R-matrix values. A summary of this analysis is shown in Table II.

For the d + d reactions, the R-matrix calculations [74] are still in progress but are approaching the final evaluation. The cross-sections, however, are already very stable and are supposed to be correct within 5% for energies of up to 1 MeV, with the uncertainty increasing to about 10% at the higher energies. The data summary for this R-matrix analysis is shown in Table III.

4.2. The new parametrization

As mentioned before, the cross-section data from the R-matrices have been fitted using the following parametrization formula:

$$\sigma = \frac{S(E)}{E \exp(B_G/\sqrt{E})} \quad (8)$$

The S-values calculated from the R-matrix cross-sections with Eq. (8) were fitted with a Padé polynomial:

$$S(E) = \frac{A1 + E(A2 + E(A3 + E(A4 + EA5)))}{1 + E(B1 + E(B2 + E(B3 + EB4)))} \quad (9)$$

TABLE II. SUMMARY OF THE ^{5}Li SYSTEM R-MATRIX ANALYSIS[a]

Channel	ℓ_{max}	a_c (fm)
d-^{3}He	3	5.0
p-^{4}He	4	2.9
p-^{4}He[a](0^-)	1	5.0

Reaction	Energy range	Number of observable types	Number of data points
^{3}He(d,d)^{3}He	E_d = 0-8 MeV	11	333
^{3}He(d,p)^{4}He	E_d = 0-8 MeV	12	651
^{4}He(p,p)^{4}He	E_p = 0-28 MeV	2	280
^{4}He(p,p)^{4}He[a](0^+)	E_p = 28 MeV	1	1
	Totals	36	1265

[a] The top part gives the maximum angular momentum quantum numbers and the channel radii used for the different channels in this system, while the bottom part summarizes the data included for each reaction.

TABLE III. SUMMARY OF THE ^{4}He SYSTEM R-MATRIX ANALYSIS[a]

Channel	ℓ_{max}	a_c (fm)
p-t	3	4.93
n-^{3}He	3	4.93
d-d	3	7.00

Reaction	Energy range	Number of observable types	Number of data points
T(p,p)T	E_p = 0-11 MeV	3	1382
T(p,n)^{3}He + inv.	E_p = 0-11 MeV	5	726
^{3}He(n,n)^{3}He	E_n = 0-10 MeV	2	126
D(d,p)T	E_d = 0-10 MeV	6	1382
D(d,n)^{3}He	E_d = 0-10 MeV	6	700
D(d,d)D	E_d = 0-10 MeV	6	336
	Totals	28	4652

[a] The top part gives the maximum angular momentum quantum numbers and the channel radii used for the different channels in this system, while the bottom part summarizes the data included for each reaction.

TABLE IV. PARAMETERS FOR THE CROSS-SECTION FIT*

Coefficient	T(d, n)^{4}He	^{3}He(d, p)^{4}He	D(d, p)T	D(d, n)^{3}He
B_G ($\sqrt{keV}$)	34.3827	68.7508	31.3970	31.3970
A1	6.927×10^4	5.7501×10^6	5.5576×10^4	5.3701×10^4
A2	7.454×10^8	2.5226×10^3	2.1054×10^2	3.3027×10^2
A3	2.050×10^6	4.5566×10^1	-3.2638×10^{-2}	-1.2706×10^{-1}
A4	5.2002×10^4	0.0	1.4987×10^{-6}	2.9327×10^{-5}
A5	0.0	0.0	1.8181×10^{-10}	-2.5151×10^{-9}
B1	6.38×10^1	-3.1995×10^{-3}	0.0	0.0
B2	-9.95×10^{-1}	-8.5530×10^{-6}	0.0	0.0
B3	6.981×10^{-5}	5.9014×10^{-8}	0.0	0.0
B4	1.728×10^{-4}	0.0	0.0	0.0
Energy range (keV)	0.5–550	0.3–900	0.5–5000	0.5–4900
$(\Delta S)_{max}$ (%)	1.9	2.2	2.0	2.5

* List of fit parameters for the fusion cross-sections, with E in keV and the cross-section calculated from Eqs (8) and (9) in units of mb.

TABLE V. TABLE OF CROSS-SECTIONS*

E (keV)	D(t, n)α (mb)	^{3}He(d, p)α (mb)	D(d, p)T (mb)	D(d, n)^{3}He (mb)
3	9.808×10^{-3}	1.119×10^{-11}	2.513×10^{-4}	2.445×10^{-4}
4	1.073×10^{-1}	1.718×10^{-9}	2.146×10^{-3}	2.093×10^{-3}
5	5.383×10^{-1}	5.199×10^{-8}	9.038×10^{-3}	8.834×10^{-3}
6	1.749×10^0	6.336×10^{-7}	2.569×10^{-2}	2.517×10^{-2}
7	4.335×10^0	4.373×10^{-6}	5.720×10^{-2}	5.616×10^{-2}
8	8.968×10^0	2.058×10^{-5}	1.081×10^{-1}	1.064×10^{-1}
9	1.632×10^1	7.374×10^{-5}	1.820×10^{-1}	1.794×10^{-1}
10	2.702×10^1	2.160×10^{-4}	2.812×10^{-1}	2.779×10^{-1}
12	6.065×10^1	1.206×10^{-3}	5.607×10^{-1}	5.563×10^{-1}
15	1.479×10^2	7.944×10^{-3}	1.180×10^0	1.178×10^0
20	4.077×10^2	6.568×10^{-2}	2.670×10^0	2.691×10^0
30	1.381×10^3	7.704×10^{-1}	6.681×10^0	6.857×10^0
40	2.817×10^3	3.266×10^0	1.116×10^1	1.165×10^1
50	4.219×10^3	8.688×10^0	1.557×10^1	1.649×10^1
60	4.984×10^3	1.788×10^1	1.971×10^1	2.115×10^1
70	4.987×10^3	3.144×10^1	2.351×10^1	2.554×10^1
80	4.545×10^3	4.978×10^1	2.698×10^1	2.964×10^1
100	3.427×10^3	1.021×10^2	3.304×10^1	3.701×10^1
120	2.576×10^3	1.768×10^2	3.812×10^1	4.343×10^1
140	2.004×10^3	2.740×10^2	4.245×10^1	4.904×10^1
150	1.792×10^3	3.303×10^2	4.438×10^1	5.160×10^1
200	1.138×10^3	6.378×10^2	5.234×10^1	6.239×10^1
250	8.135×10^2	8.122×10^2	5.831×10^1	7.071×10^1
300	6.234×10^2	7.731×10^2	6.302×10^1	7.732×10^1
400	4.126×10^2	5.304×10^2	7.005×10^1	8.702×10^1

* Cross-sections for all the reactions as a function of the energy in the CM frame. These values were calculated from Eqs (8) and (9) with the parameters from Table IV.

However, not all of these coefficients were necessary in all cases. The results of the fit procedure are given in Table IV together with the Gamov constant B_G for each of the reactions. With E in keV, the fusion cross-sections are given in units of millibarn (1 mb = 10^{-27} cm^2). The two bottom lines of Table IV show the energy range in which the parametrizations are valid, and also the maximum deviation of the approximations from the original R-matrix cross-sections. Table V lists for the four reactions the cross-sections calculated with this fit as a function of the energy in the CM frame.

For the non-resonant reactions, a single set of parameters was found which describes sufficiently well the data over the whole energy range (up to about 5 MeV), but for the resonant reactions T(d,n)^{4}He and ^{3}He(d,p)^{4}He no such set was found. The validity range for these reactions is very restricted, as Table IV shows. Therefore, we calculated a second parameter set for these reactions which describes the cross-sections at higher energies. These fit parameters are shown in Table VI. For most applications, however, the 'low energy' fit from Table IV will be sufficient. Even for burnup calculations, where tritons start with an energy of 1.08 MeV (E = 430 keV) and ^{3}He ions start with 820 keV (E = 330 keV), this fit is valid for the whole energy range needed.

TABLE VI. PARAMETERS FOR THE HIGH ENERGY CROSS-SECTION FIT[a]

Coefficient	T(d,n)^{4}He	^{3}He(d,p)^{4}He
B_G ($\sqrt{keV}$)	34.3827	68.7508
A1	-1.4714×10^{6}	-8.3993×10^{5}
B1	-8.4127×10^{-3}	-2.6830×10^{-3}
B2	4.7983×10^{-6}	1.1633×10^{-6}
B3	-1.0748×10^{-9}	-2.1332×10^{-10}
B4	8.5184×10^{-14}	1.4250×10^{-14}
Energy range (keV)	550-4700	900-4800
$(\Delta S)_{max}$ (%)	2.5	1.2

[a] Fit parameters for the very high energy range for the resonant fusion cross-sections, with E in keV and the cross-section calculated from Eqs (8) and (9) in units of mb.

If one has to use both formulas to cover the energy range of interest, one has to take care with the transition of one fit to the other. For the T(d,n)^{4}He reaction, the low energy fit reproduces the R-matrix value exactly at 500 keV, and at 550 keV it is about 1.5% lower. The high energy fit is about 1.3% lower than the R-matrix value at 500 keV and about 0.8% lower at 550 keV. Both fits agree with each other at 530 keV, which is the best point to use in order to obtain a smooth transition between the formulas.

The situation is different for the ^{3}He(d,p)^{4}He reaction, where the low energy fit reproduces the R-matrix data at 760 keV. At higher energies it is smaller, and the difference increases to 2.2% at 900 keV. At this energy, the high energy fit is 1.1% above the R-matrix data and it reproduces these input data at about 1000 keV. This means that the transition from one formula to the other, although discontinuous, is best made at exactly 900 keV. More details on these calculations and the deviations from the input data have been documented in Ref. [17].

4.3. Comparison with the old parametrizations and tables

Figures 16-19 show for comparison the ratio of the cross-section given by different approximation formulas to the cross-section from the R-matrix calculations. For the resonant reactions, a detailed comparison is only done for the 'low energy' fit from Table IV. All of the figures displayed here show very clearly the systematic deviation of Duane's approximation formula at low energies.

For the T(d,n)^{4}He reaction, Peres' formula is up to 17% too low at energies below about 5 keV (or $E_d \approx 8.3$ keV), but it is correct within 5% for ener-

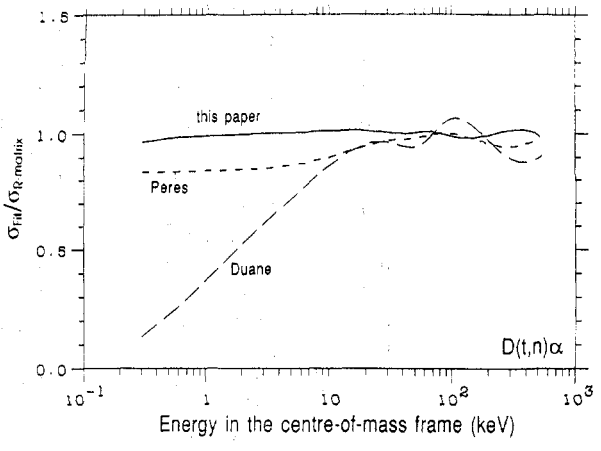

FIG. 16. Comparison of the cross-sections calculated from the approximation formulas with the data from the R-matrix for the T(d,n)^{4}He reaction. The solid line shows the fit presented in this paper.

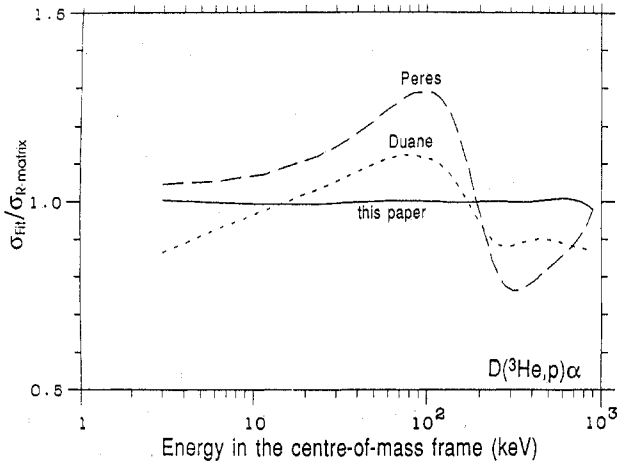

FIG. 17. Comparison of the cross-sections calculated from the approximation formulas with the data from the R-matrix for the $D(^3He,p)^4He$ reaction. The steep variation of the cross-section ratio for Duane's and Peres' fit are a consequence of the fact that their formulas had the resonance at a lower energy than the R-matrix does.

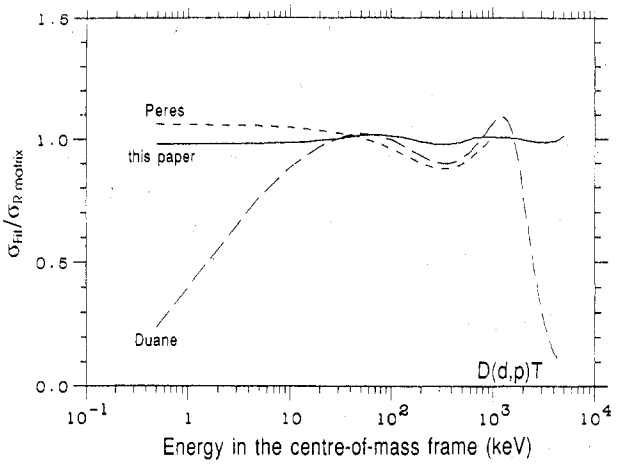

FIG. 18. Comparison of the cross-sections calculated from the approximation formulas with the data from the R-matrix for the D(d,p)T reaction.

gies above about 20 keV. Duane's formula has deviations of up to 13% even for higher energies.

As mentioned in connection with Figs 5–8 for the $^3He(d,p)^4He$ reaction, the maximum in the old parametrizations occurs at a lower energy than in the R-matrix evaluation. This can be seen very nicely in Fig. 17, where both fits are much higher than the R-matrix values for energies below about 200 keV, but are too low for energies above 200 keV. For this reaction, the maximum deviation of Peres' fit (30%) is even higher than the deviation of Duane's fit ($\approx$12%).

For the D(d,p)T reaction (Fig. 18), Peres' fit (which is only valid for E $\leq$ 1000 keV) is about 8% too high for energies below 10 keV and about 12% too low for energies between 200 and 400 keV. Duane's fit, however, is not usable for energies below about 10 keV, but is only up to 12% too low for energies between 10 and 100 keV. Above 1 MeV, the fit again drops very rapidly.

With respect to Duane's fit, the situation is similar for the $D(d,n)^3He$ reaction (Fig. 19). Peres' parametrization, however, agrees very well with the R-matrix results for energies below about 10 keV. Above this value, his parametrization is too low, with a maximum deviation of about 25% at E = 250 keV.

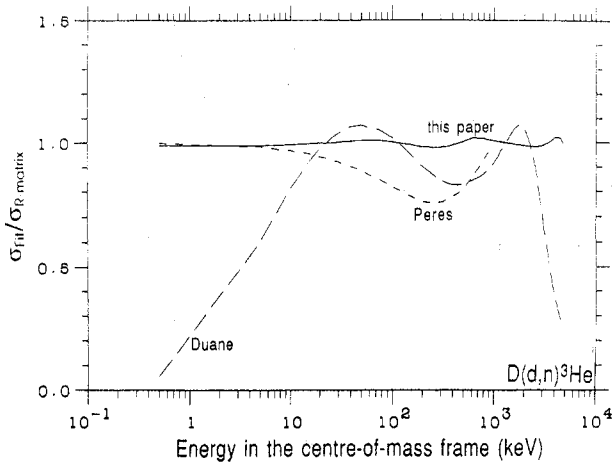

FIG. 19. Comparison of the cross-sections calculated from the approximation formulas with the data from the R-matrix for the $D(d,n)^3He$ reaction.

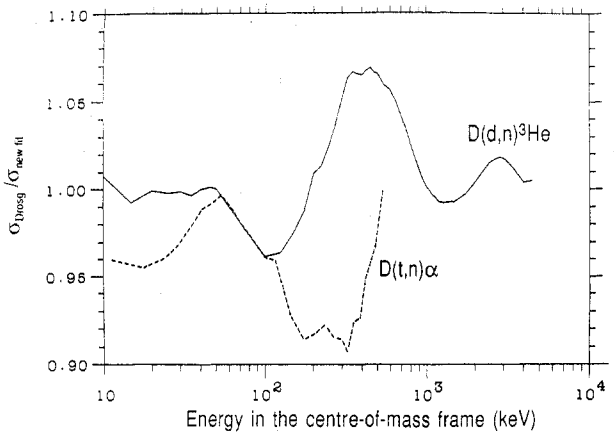

FIG. 20. Comparison of the cross-sections from Drosg's spline fit [68] for both of the neutron producing reactions with the new approximation formula presented in this paper.

In general, the deviations of the old parametrizations from the R-matrix cross-sections are much larger than the cross-section uncertainties and the deviations of the new approximation formulas.

Tables with data from a spline fit to the experimental data have also been published for the neutron producing reactions D(d,n)^{3}He and T(d,n)^{4}He [36, 68]. Drosg and Schwerer [68] used the same data as Liskien and Paulsen [36], and, for the T(d,n)^{4}He reaction, also the most recent Los Alamos data [19, 43]. We therefore compare in Fig. 20 our new fit formula only with this newer data table.

5. REACTIVITY PARAMETRIZATION

The fusion rate depends on the relative velocity of the reacting particles, and, since in a plasma the ions have not a single velocity but a velocity distribution, the fusion rate per volume dR/dV is proportional to the fusion reactivity $\langle\sigma v\rangle$:

$$dR/dV = \frac{n_i n_j}{1+\delta_{ij}} \langle\sigma v\rangle \tag{10}$$

where n_i, n_j are the particle densities and δ_{ij} is the Kronecker symbol. With $f(\vec{v}_i)$ the velocity distribution of a particle and g the relative velocity ($\vec{g} = \vec{v}_i - \vec{v}_j$), we obtain

$$\langle\sigma v\rangle = \int\int f(\vec{v}_i)\, f(\vec{v}_j)\, \sigma(|g|)\, |g|\, d\vec{v}_i\, d\vec{v}_j \tag{11}$$

This is a sixfold integral, but in some cases it can be reduced to a simpler integral by symmetry considerations [75]; also, approximation formulas for this integral have been derived analytically, for Maxwellian ion energy distributions [15] as well as for beam–target reactivities [16, 75]. These formulas, however, are not very convenient and are not accurate enough for most applications. For the T(d,n)^{4}He and ^{3}He(d,p)^{4}He reactions, also a full calculation of the Fokker–Planck equation has been used to evaluate the reactivities [76]. Such numerical calculations are also necessary to evaluate the influence of fast ion tails from neutral beam heating and ion cyclotron resonance heating that can significantly increase the fusion reactivity [77].

For thermal plasmas, however, where the ions have a Maxwellian energy distribution, the thermal reactivity can be accurately calculated numerically, and such data have been published quite often.

5.1. Status of the parametrizations

At the beginning of fusion research, graphical data [78, 79] and tabulated reactivity data [80] for thermal plasmas were published. These reactivities had been numerically integrated from cross-section data in the early reviews [81]. As the database of the cross-sections grew, quite a number of reports on reactivities were published [82], often as internal reports; we apologize for any omissions of these in our discussion.

Later, analytical expressions for thermal reactivities were presented by, among others, Peres [3], Hively et al. [4, 5], Brunelli [83], and Brueckner and Jorna [84]. The latter three parametrizations, which have been widely used, are based on Duane's [1] cross-section formulas. Johner [85] calculated a very crude (monomial) approximation for the T(d,n)^{4}He reaction based on Peres' cross-section formula. Slaughter [86] calculated reactivities for a variety of ion energy distributions and also parametrized his results.

Recently, Sadler and Van Belle [18] used a simplified R-matrix description for the T(d,n)^{4}He cross-section alone to derive new parametrizations of the cross-sections and thermal reactivities. This is similar to what we have done here, except that we have obtained the cross-section values directly from the multilevel R-matrix parameters of the final multichannel ^{5}He analysis.

Since all previous reactivity evaluations use the old cross-section parametrizations (or simplified R-matrix results) that do not represent the cross-sections well enough, as we have seen, it seems necessary to calculate new reactivities on the basis of the cross-sections calculated from the final R-matrix parameters.

5.2. The new parametrization

We calculated thermal reactivities numerically on the basis of the new R-matrix cross-sections and we used these reactivities to calculate a new parametrization. For this parametrization we used the functional form proposed by Peres [3]:

$$\langle\sigma v\rangle = C1 \cdot \theta \sqrt{\xi/(m_r c^2 T^3)}\, e^{-3\xi} \tag{12}$$

$$\theta = T \Big/ \left[1 - \frac{T(C2 + T(C4 + TC6))}{1 + T(C3 + T(C5 + TC7))} \right] \tag{13}$$

$$\xi = (B_G^2/(4\theta))^{1/3} \tag{14}$$

The parameters resulting from this fit are shown in Table VII. The reactivity $\langle\sigma v\rangle$ is in cm^3/s when T is the ion temperature in keV. Table VIII lists the values calculated with this fit as a function of ion temperature for all the reactions.

The fits for the d + t and d + d reactions are valid for ion temperatures of 0.2 keV $\leq T_i \leq$ 100 keV, and the maximum deviation of the fit formula from the input

TABLE VII. PARAMETERS FOR THE REACTIVITY FIT*

Coefficient	$T(d,n)^4He$	$^3He(d,p)^4He$	$D(d,p)T$	$D(d,n)^3He$
B_G ($\sqrt{keV}$)	34.3827	68.7508	31.3970	31.3970
m_rc^2 (keV)	1 124 656	1 124 572	937 814	937 814
C1	1.17302×10^{-9}	5.51036×10^{-10}	5.65718×10^{-12}	5.43360×10^{-12}
C2	1.51361×10^{-2}	6.41918×10^{-3}	3.41267×10^{-3}	5.85778×10^{-3}
C3	7.51886×10^{-2}	-2.02896×10^{-3}	1.99167×10^{-3}	7.68222×10^{-3}
C4	4.60643×10^{-3}	-1.91080×10^{-5}	0.0	0.0
C5	1.35000×10^{-2}	1.35776×10^{-4}	1.05060×10^{-5}	-2.96400×10^{-6}
C6	-1.06750×10^{-4}	0.0	0.0	0.0
C7	1.36600×10^{-5}	0.0	0.0	0.0
T_i range (keV)	0.2–100	0.5–190	0.2–100	0.2–100
$(\Delta \langle \sigma v \rangle)_{max}$ (%)	0.25	2.5	0.35	0.3

* List of the fit parameters for the fusion reactivity in Maxwellian plasmas. T_i is in keV and the reactivity is in cm^3/s. The bottom lines show the validity range of this fit and the maximum deviation of the fit from the input data.

TABLE VIII. THERMAL REACTIVITIES FOR ALL REACTIONS AS A FUNCTION OF THE ION TEMPERATURE

T_i (keV)	$D(t,n)\alpha$ (cm^3/s)	$^3He(d,p)\alpha$ (cm^3/s)	$D(d,p)T$ (cm^3/s)	$D(d,n)^3He$ (cm^3/s)
0.2	1.254×10^{-26}	1.414×10^{-35}	4.640×10^{-28}	4.482×10^{-28}
0.3	7.292×10^{-25}	1.033×10^{-32}	2.071×10^{-26}	2.004×10^{-26}
0.4	9.344×10^{-24}	6.537×10^{-31}	2.237×10^{-25}	2.168×10^{-25}
0.5	5.697×10^{-23}	1.241×10^{-29}	1.204×10^{-24}	1.169×10^{-24}
0.6	2.253×10^{-22}	1.166×10^{-28}	4.321×10^{-24}	4.200×10^{-24}
0.7	6.740×10^{-22}	6.960×10^{-28}	1.193×10^{-23}	1.162×10^{-23}
0.8	1.662×10^{-21}	3.032×10^{-27}	2.751×10^{-23}	2.681×10^{-23}
1.0	6.857×10^{-21}	3.057×10^{-26}	1.017×10^{-22}	9.933×10^{-23}
1.3	2.546×10^{-20}	3.708×10^{-25}	3.387×10^{-22}	3.319×10^{-22}
1.5	6.923×10^{-20}	1.317×10^{-24}	8.431×10^{-22}	8.284×10^{-22}
1.8	1.539×10^{-19}	6.053×10^{-24}	1.739×10^{-21}	1.713×10^{-21}
2.0	2.977×10^{-19}	1.399×10^{-23}	3.150×10^{-21}	3.110×10^{-21}
2.5	8.425×10^{-19}	7.477×10^{-23}	7.969×10^{-21}	7.905×10^{-21}
3.0	1.867×10^{-18}	2.676×10^{-22}	1.608×10^{-20}	1.602×10^{-20}
4.0	5.974×10^{-18}	1.710×10^{-21}	4.428×10^{-20}	4.447×10^{-20}
5.0	1.366×10^{-17}	6.377×10^{-21}	9.024×10^{-20}	9.128×10^{-20}
6.0	2.554×10^{-17}	1.739×10^{-20}	1.545×10^{-19}	1.573×10^{-19}
8.0	6.222×10^{-17}	7.504×10^{-20}	3.354×10^{-19}	3.457×10^{-19}
10.0	1.136×10^{-16}	2.126×10^{-19}	5.781×10^{-19}	6.023×10^{-19}
12.0	1.747×10^{-16}	4.715×10^{-19}	8.723×10^{-19}	9.175×10^{-19}
15.0	2.740×10^{-16}	1.175×10^{-18}	1.390×10^{-18}	1.481×10^{-18}
20.0	4.330×10^{-16}	3.482×10^{-18}	2.399×10^{-18}	2.603×10^{-18}
30.0	6.681×10^{-16}	1.363×10^{-17}	4.728×10^{-18}	5.271×10^{-18}
40.0	7.998×10^{-16}	3.160×10^{-17}	7.249×10^{-18}	8.235×10^{-18}
50.0	8.649×10^{-16}	5.554×10^{-17}	9.838×10^{-18}	1.133×10^{-17}

data is shown in the last line of the table. This is the most interesting temperature interval for these reactions, but, for the ^{3}He(d,p)^{4}He reaction, higher temperatures are important. Therefore, this fit has been calculated for ion temperatures 0.5 keV $\leq T_i \leq$ 195 keV. The maximum deviation between input data and fit formula is much larger than that for the other reactions (and for the fit presented in Ref. [17]), but, since the absolute uncertainties for the ^{3}He(d,p)^{4}He reactivities calculated from R-matrix cross-sections are 10% anyway, the inaccuracy of the fit does not significantly increase the total error of the parametrization, which is about 10%.

The absolute uncertainties for the reactivities calculated for the R-matrix cross-sections are 3% for the d + t reaction and 6% for the d + d reactions. Since the errors of the corresponding fits are negligible, these values are also the total errors of our parametrization.

5.3. Comparison with the old parametrizations

Next we compare this parametrization as well as the old formulas with the numerically calculated reactivity values which have been the input for our fit. Figure 21 shows this comparison for the T(d,n)^{4}He reaction as the ratio of the values calculated from the fit formulas to the input data. Hively [4, 5] and Brunelli [83] used the reactivity data that Miley et al. [87] calculated from Duane's cross-section formulas [1]. The curve labelled HIVELY '77 was calculated from Eq. (5) in Hively's 1977 paper [4]. All three of these parametrizations show large deviations from the correct reactivities for low ion temperatures, as one would expect from the fact that Duane's cross-section formulas were used. Peres' formula [3] is about 15% too low at T_i = 1 keV but only 2% too low for T_i > 10 keV. The parametrization of Sadler et al. [88], which is based on intermediate R-matrix results [19], is only about 5% too low between 1 and 10 keV, but above 20 keV the deviation increases to about 10% at 100 keV.

Figure 22 shows the same comparison for the ^{3}He(d,p)^{4}He reaction. The problems seen in Figs 5–8 with the cross-section formulas are also reflected in the reactivity parametrizations. The deviations are quite large and they even change sign.

For the D(d,p)T reaction shown in Fig. 23 the parametrization of Peres [3] is always better than 10%, but again the formulas based on Duane's data [1] have quite large deviations. In Fig. 24 the comparison for the D(d,n)^{3}He reaction shows the same situation for Hively's formulas, but Peres' formula has a much larger deviation (up to about 20%) for high ion temperatures.

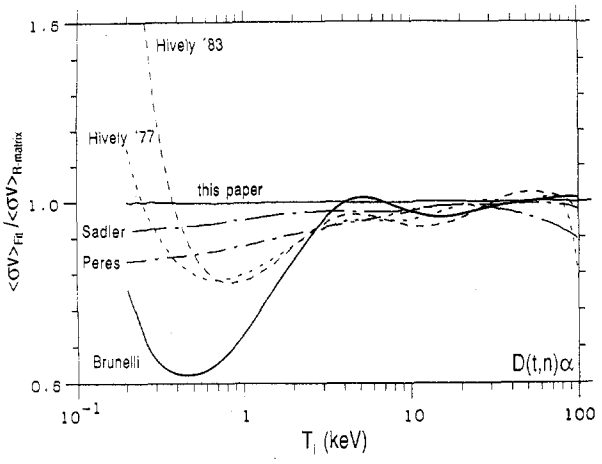

FIG. 21. Comparison of different ⟨σv⟩ fit formulas with the reactivity values calculated from the R-matrix cross-sections for the T(d,n)^{4}He reaction. For the curve labels see text.

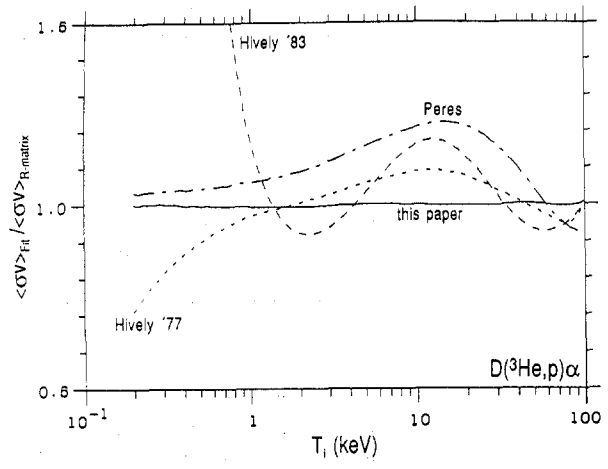

FIG. 22. Comparison of different ⟨σv⟩ fit formulas for the D(^{3}He,p)^{4}He reaction with the reactivity values calculated from the R-matrix cross-sections.

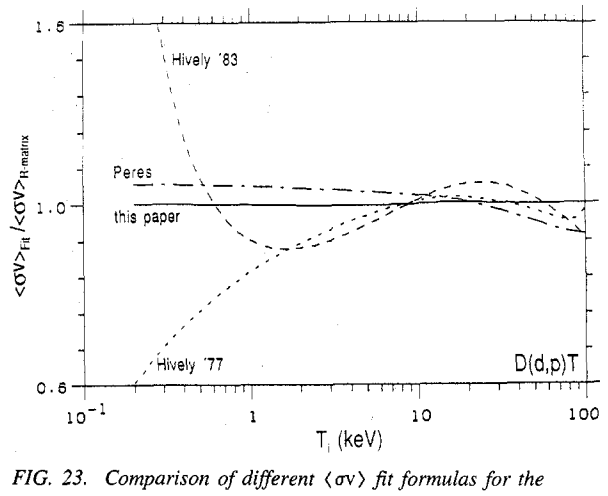

FIG. 23. Comparison of different ⟨σv⟩ fit formulas for the D(d,p)T reaction with the reactivity values calculated from the R-matrix cross-sections.

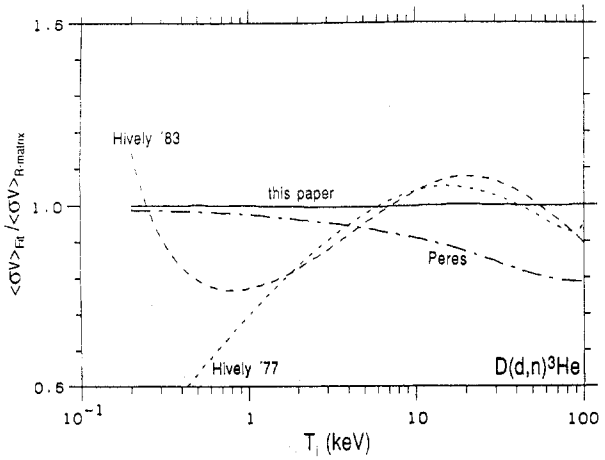

FIG. 24. Comparison of different ⟨σv⟩ fit formulas for the D(d,n)^{3}He reaction with the reactivity values calculated from the R-matrix cross-sections.

6. BRANCHING RATIOS FOR THE d + d REACTION

Not only are the absolute values of the fusion cross-sections and reactivities important for fusion research, but, for some applications, the branching ratio BR = $\sigma_{ddp}/\sigma_{ddn}$ of the cross-sections for the proton branch and the neutron branch of the d + d reaction is also important, for the following reasons:

(1) In triton burnup measurements the source rate of the tritons from the D(d,p)T reaction has to be known, but, normally, only the emission rate of the neutrons from the D(d,n)^{3}He reaction is measured and used. Generally, this difference in the emission rates has been neglected, but recently [89] it was argued that these rates can differ by about 15% in the case of TFTR.

(2) If one tries to determine the fusion emission profile by measuring charged fusion products such as the 3 MeV proton along a line of sight and comparing this flux with the absolutely measured total neutron yield [90], the difference in yield from the different branches has to be taken into account.

It has been shown in the preceding sections that the old approximation formulas for the cross-sections and reactivities are not adequate for today's needs, and the situation is equally bad, or even worse, for the branching ratio calculated from these approximations. Therefore, we compare the branching ratio for the cross-sections (BR = $\sigma_{ddp}/\sigma_{ddn}$) and the branching ratio for the Maxwellian reactivities (BRSV = $\langle\sigma v\rangle_{ddp}/\langle\sigma v\rangle_{ddn}$) calculated from all the approximation formulas with the values obtained directly from the ^{4}He R-matrix analysis.

6.1. Branching ratio for the fusion cross-sections

Figure 25(a) compares the branching ratio calculated from the cross-section approximations of Duane [1] and Peres [3] and from the one given in this paper with the values that result directly from the R-matrix analysis [91]. The results of this Coulomb corrected, charge independent analysis of the A = 4 reactions agree very well with the most recent d + d measurements [50, 54, 92, 93]. It can clearly be seen that the branching ratio departs from unity and that it decreases at higher energies. The branching ratio calculated from the old formulas, however, does not represent this correctly. The cross-section formulas from Duane give a completely wrong low energy behaviour, as mentioned earlier, and Peres' formulas result in a branching ratio that is always about 10% too high. The cross-section approximation presented in this paper gives a branching ratio very close (about 1% maximum deviation) to

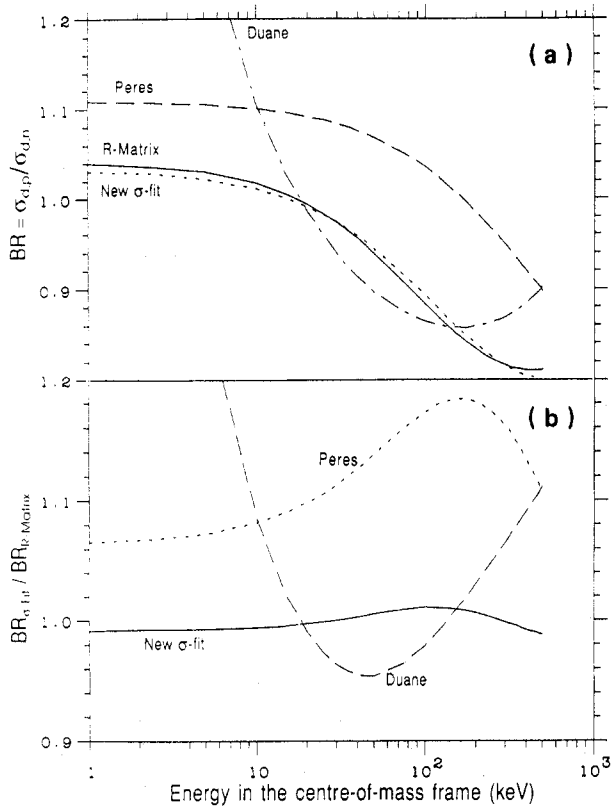

FIG. 25. (a) Branching ratio for the d + d reactions as a function the the CM energy. The broken lines have been calculated from different approximation formulas. The solid line is the branching ratio as it is given by the R-matrix results directly.
(b) Ratio of the branching ratios calculated from approximation formulas to the R-matrix branching ratios, demonstrating that the old formulas do not adequately represent the branching ratio.

the R-matrix data. This can also be seen in Fig. 25(b), where the ratio of these branching ratios (calculated from the old approximation formulas) to the branching ratio from the R-matrix is shown.

For cases where the absolute cross-sections are not needed, but rather the branching ratio itself, the R-matrix result can be approximated by a simple polynomial:

$$BR_{fit} = 1.04305 - 2.6573 \times 10^{-3}E + 1.2923 \times 10^{-5}E^2 - 2.4454 \times 10^{-8}E^3 \quad (15)$$

For energies between 0.5 keV and 200 keV, the deviation of BR_{fit} from the R-matrix branching ratio is always smaller than 0.15%.

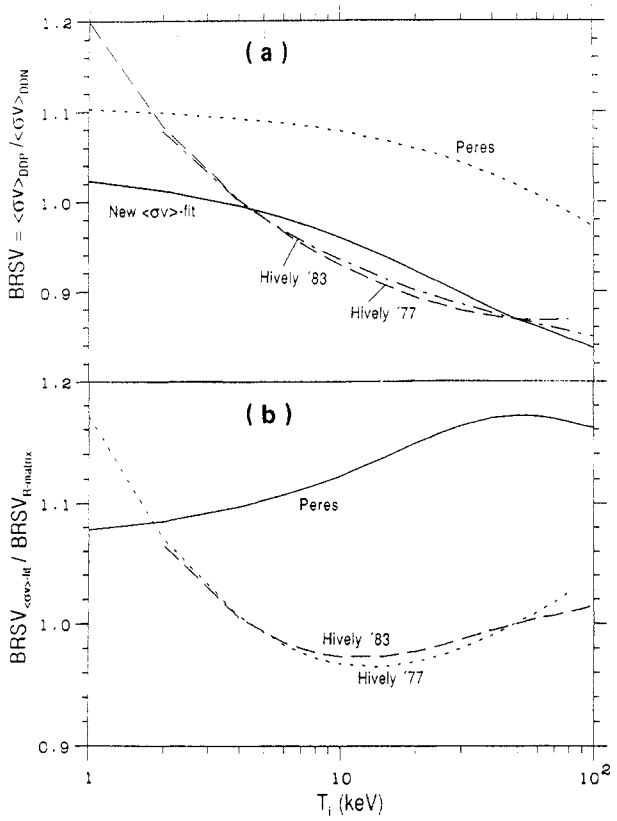

FIG. 26. (a) Branching ratio of the Maxwellian reactivities for the d + d reactions as a function of the CM energy. BRSV is the ratio of the reactivities calculated from the approximation formulas of Hively and Peres, and of the one presented in this paper (which approximates the R-matrix reactivities and therefore also BRSV to better than 0.5%).
(b) Ratio of the branching ratios from the old approximation formulas to the branching ratio from the new reactivity formulas presented in this paper, demonstrating that again Peres' formulas give a branchign ratio that is always too high, while Hively's formulas are almost correct above about 10 keV.

6.2. Branching ratio for the fusion reactivities

For thermal plasmas, the branching ratio BRSV of the Maxwellian reactivities is again important, and this branching ratio (as calculated from different reactivity formulas) is shown in Fig. 26(a). Since the reactivities from the new approximation formula presented in Table VII represent the R-matrix reactivities to better than 0.35%, the branching ratio calculated from this new reactivity fit represents the R-matrix branching ratio to at least better than 0.7%. Therefore, the BRSV values obtained directly from the R-matrix have been omitted in this figure.

Qualitatively, the situation is similar to that illustrated in Fig. 25, with Peres' values always being too high and Hively's data (which are based on Duane's data) being nearly correct for ion temperatures above about 2 keV. Figure 26(b) again shows the ratio of the BRSV values from the old formulas to the values from our new formula (which are practically identical to the values from the R-matrix).

For cases where only the branching ratio BRSV is needed, rather than the absolute reactivities, the values from the new reactivity parametrization can also be approximated by a simple polynomial:

$$BRSV_{fit} = 1.02934 - 8.3264 \times 10^{-3}T_i + 1.7631 \times 10^{-4}T_i^2 - 1.8201 \times 10^{-6}T_i^3 + 6.9855 \times 10^{-9}T_i^4 \quad (16)$$

For ion temperatures between 0.5 keV and 200 keV, the deviation of $BRSV_{fit}$ from the R-matrix branching ratio is always smaller than 0.5%.

6.3. Consequences of the d + d branching ratio differences in fusion plasmas

Using Eq. (16), we find that for ion temperatures of the order of 30 keV the yield of tritons is about 10% lower than the neutron yield (while Hively gives a value of about 12% and Peres claims that it is 4% higher). For beam–target reactions (which means typically E = 50 keV in TFTR and E = 40 keV in JET) the triton yield according to Eq. (15) is 6% (4% in JET) lower than the neutron yield, while Duane's data result in a 10% (9%) effect and Peres' formulas give 7% (8%) more tritons than neutrons.

Depending on the plasma conditions (and the relative importance of thermal and beam–target reactions), the branching ratio will result in a triton yield that is different from the neutron yield, but this effect is much smaller than claimed recently [89] on the basis

of Duane's cross-section parametrization, and it will probably be of the order of about 8%.

For thermal ASDEX plasmas the triton yield is only 1–2% higher than the neutron yield (Peres: 10% higher, Hively: 8–20% higher), and this difference is negligible.

7. SUMMARY

It has been shown that the parametrization formulas for the cross-sections of the reactions T(d,n)^{4}He, ^{3}He(d,p)^{4}He, D(d,p)T and D(d,n)^{3}He no longer represent adequately the present status of the experimental data and the best evaluations of these data. New experimental measurements and the use of R-matrix theory have resulted in cross-section data with much higher accuracy leading to much better parametrizations.

On the basis of these cross-section data, reactivities for thermal plasmas have been calculated numerically, and new parametrizations have been presented for the cross-sections and the reactivities.

As this paper was nearly complete, we became aware of two other recent evaluations of the fusion cross-sections, one done at Lawrence Livermore National Laboratory [94] and the other in the Russian Federation [95]. These evaluations are largely based on mathematical, rather than physical, representations of the experimental data (although the Livermore evaluation uses a single-level R-matrix calculation to give low energy T(d,n)^{4}He and ^{3}He(d,p)^{4}He cross-sections). Since these new evaluations took the recent data into account, they are presumably in better agreement with our evaluations than are the older ones, but a detailed comparison will have to be done in the future.

ACKNOWLEDGEMENTS

The authors acknowledge the useful discussions and contributions made by U. Schumacher, B. Bomba and G. Sadler (JET). Thanks are also due to O.J.W.F. Kardaun for help with SAS, to J. Murphy (PPPL) for making the use of LOCUS possible at IPP, and to H. Volkenandt for help in preparing the numerous figures.

REFERENCES

[1] DUANE, B.H., "Fusion cross section theory", in Annual Report on CTR Technology 1972 (WOLKENHAUER, W.C., Ed.), Rep. BNWL-1685, Battelle Pacific Northwest Laboratory, Richland, WA (1972).

[2] BOOK, D.L., NRL plasma formulary, Publ. 0084-4040, Rev., Naval Research Laboratory, Washington, DC (1987).

[3] PERES, A.J., J. Nucl. Mater. **50** (1979) 5569.

[4] HIVELY, L.M., Nucl. Fusion **17** (1977) 873.

[5] HIVELY, L.M., Nucl. Technol./Fusion **3** (1983) 199.

[6] HALE, G., DODDER, D.C., in Nuclear Cross Sections for Technology (Proc. Int. Conf. Knoxville, TN, 1979), NBS special publication 594, National Bureau of Standards, Washington, DC (1980) 650.

[7] BRENNAN, J.G., Phys. Rev. **111** (1958) 1592.

[8] FICK, D., WEISS, U., Z. Phys. **265** (1973) 87.

[9] FIARMAN, S., MEYERHOF, W.E., Nucl. Phys., A **206** (1973) 1.

[10] AJZENBERG-SELOVE, F., Nucl. Phys., A **490** (1988) 1.

[11] GAMOV, G., Z. Phys. **51** (1928) 204.

[12] BURBIDGE, E.M., BURBIDGE, G.R., FOWLER, W.A., HOYLE, F., Rev. Mod. Phys. **29** (1957) 547.

[13] CLAYTON, D.D., Principles of Stellar Evolution and Nucleosynthesis, McGraw-Hill, New York (1968).

[14] SCHIFF, L.I., Quantum Mechanics, 1st edn, McGraw-Hill, New York (1949) 117.

[15] BAHCALL, J.N., Astrophys. J. **143** (1966) 259.

[16] MIKKELSEN, D.R., Nucl. Fusion **29** (1989) 1113.

[17] BOSCH, H.-S., Review of Data and Formulas for Fusion Cross-sections, Tech. Rep. I/252, Max-Planck-Institut für Plasmaphysik, Garching (1990).

[18] SADLER, G., Van BELLE, P., An Improved Formulation of the D(t,n)^{4}He Reaction Cross-section, Tech. Rep. JET-IR(87)08, JET Joint Undertaking, Abingdon, Oxfordshire (1987).

[19] JARMIE, N., BROWN, R.E., HARDEKOPF, R.A., Phys. Rev., C **29** (1984) 2031; Erratum: Phys. Rev., C **33** (1986) 385.

[20] WIGNER, E.P., EISENBUD, L., Phys. Rev. **72** (1947) 29.

[21] LANE, A.M., THOMAS, R.G., Rev. Mod. Phys. **30** (1958) 257.

[22] HALE, G.M., BROWN, R.E., JARMIE, N., Phys. Rev. Lett. **59** (1987) 763; Comment: Phys. Rev. Lett. **59** (1987) 2818.

[23] TILLEY, D.R., WELLER, H.R., HALE, G.M., Energy levels of light nuclei, A = 4, to be published in Nucl. Phys., A.

[24] HALE, G.M., Data for Fusion Reactions, LASL Memo T-2-L-3360, updated version, Los Alamos Scientific Laboratory, Los Alamos, NM (1986).

[25] HALE, G.M., d–t Cross Section and Reaction Rate, LANL Memo T-2-M-1767, Los Alamos National Laboratory, Los Alamos, NM (1986).

[26] BROLLEY, J.E., Jr., FOWLER, J.L., STOVALL, E.J., Jr., Phys. Rev. **82** (1951) 502.

[27] ARGO, H.V., TASCHEK, R.F., AGNEW, H.M., HEMMENDINGER, A., LELAND, W.T., Phys. Rev. **87** (1952) 612.

[28] CONNER, J.P., BONNER, T.W., SMITH, J.R., Phys. Rev. **88** (1952) 468.

[29] STRATTON, T.F., FREIER, G.D., Phys. Rev. **88** (1952) 261.

[30] ARNOLD, W.R., PHILLIPS, J.A., SAWYER, G.A., STOVALL, E.J., Jr., TUCK, J.L., Phys. Rev. **93** (1954) 483.

[31] HEMMENDINGER, A., ARGO, H.V., Phys. Rev. **98** (1955) 70.
[32] BAME, S.J., Jr., PERRY, J.E., Jr., Phys. Rev. **107** (1957) 1616.
[33] ARNOLD, W.R., PHILLIPS, J.A., SAWYER, G.A., STOVALL, E.J., Jr., TUCK, J.L., Absolute Cross Section for the Reaction T(d,n)He^4 from 10 to 120 keV, Tech. Rep. LA-1479, Los Alamos Scientific Laboratory, Los Alamos, NM (1953).
[34] JARVIS, R.G., ROAF, D., Proc. R. Soc. (London), Ser. A **218** (1953) 432.
[35] SMITH, J.R., THORNTON, S.T., Nucl. Phys., A **187** (1972) 433.
[36] LISKIEN, H., PAULSEN, A., Nucl. Data Tables **11** (1973) 569.
[37] GALONSKY, A., JOHNSON, C.H., Phys. Rev. **104** (1956) 421.
[38] BALABANOV, E.M., BARIT, I.I., KATSAUROV, L.N., FRANK, I.M., SHTRANIKH, I.V., Sov. J. At. Energy, Suppl. No. 5 (1957) 43.
[39] GOLDBERG, M.D., LeBLANC, J.M., Phys. Rev. **122** (1961) 164.
[40] KOBZEV, A.P., SALATSKIJ, V.L., TELEZHNIKOV, S.A., Yad. Fiz. **3** (1966) 1060; Sov. J. Nucl. Phys. **3** (1966) 774.
[41] KATSAUROV, L.N., Tr. Fiz. Inst., Akad. Nauk SSSR **14** (1962) 224.
[42] JARMIE, N., BROWN, R.E., HARDEKOPF, R.A., in Nuclear Data for Science and Technology (Proc. Int. Conf. Antwerpen, 1982), Reidel, Dordrecht (1983) 318.
[43] BROWN, R.E., JARMIE, N., HALE, G.M., Phys. Rev., C **35** (1987) 1999; Erratum: Phys. Rev., C **36** (1987) 1220.
[44] BRETSCHER, E., FRENCH, A.P., Phys. Rev. **75** (1949) 1154.
[45] BONNER, T.W., CONNER, J.P., LILLIE, A.B., Phys. Rev. **88** (1952) 473.
[46] KUNZ, W.E., Phys. Rev. **97** (1955) 456.
[47] YARNELL, J.L., LOVBERG, R.H., STRATTON, W.R., Phys. Rev. **90** (1953) 292.
[48] FREIER, G., HOLMGREN, H., Phys. Rev. **93** (1954) 825.
[49] MÖLLER, W., BESENBACHER, F., Nucl. Instrum. Methods **168** (1980) 111.
[50] KRAUSS, A., BECKER, H.W., TRAUTVETTER, H.P., ROLFS, C., BRAND, K., Nucl. Phys., A **465** (1987) 150.
[51] ALLRED, J.C., Phys. Rev. **84** (1951) 695.
[52] THEUS, R.B., McGARRY, W.I., BEACH, L.A., Nucl. Phys., A **80** (1966) 273.
[53] POSPIECH, G., GENZ, H., MARLINGHAUS, E.H., RICHTER, A., SCHRIEDER, G., Nucl. Phys., A **239** (1975) 125.
[54] BROWN, R.E., JARMIE, N., Phys. Rev., C **41** (1990) 1391.
[55] BLAIR, J.M., FREIER, G., LAMPI, E., SLEATOR, W., Jr., WILLIAMS, J.H., Phys. Rev. **74** (1948) 1599.
[56] MOFFAT, J., ROAF, D., SANDERS, J.H., Proc. R. Soc. (London), Ser. A **212** (1952) 220.
[57] DAVENPORT, P.A., JEFFRIES, T.O., OWEN, M.E., PRICE, F.V., ROAF, D., Proc. R. Soc. (London), Ser. A **216** (1953) 66.
[58] ELIOT, E.A., ROAF, D., SHAW, P.F.D., Proc. R. Soc. (London), Ser. A **216** (1953) 57.
[59] PRESTON, G., SHAW, P.F.D., YOUNG, S.A., Proc. R. Soc. (London), Ser. A **226** (1954) 206.
[60] McNEILL, K.G., KEYSER, G.M., Phys. Rev. **81** (1951) 602.
[61] WENZEL, W.A., WHALING, W., Phys. Rev. **88** (1952) 1149.
[62] BOOTH, D.L., PRESTON, G., SHAW, P.F.D., Proc. R. Soc. (London), Ser. A **69** (1956) 265.
[63] BROLLEY, J.E., Jr., PUTNAM, T.M., ROSEN, L., Phys. Rev. **107** (1957) 820.
[64] SCHULTE, R.L., COSACK, M., OBST, A.W., WEIL, J.L., Nucl. Phys., A **192** (1972) 609.
[65] JARMIE, N., BROWN, R.E., Nucl. Instrum. Methods Phys. Res., Sect. B **10/11** (1985) 405.
[66] ERICKSON, K.W., FOWLER, J.L., STOVALL, E.J., Jr., Phys. Rev. **76** (1949) 1141.
[67] HUNTER, G.T., RICHARDS, H.T., Phys. Rev. **76** (1949) 1445.
[68] DROSG, M., SCHWERER, O., in Handbook on Nuclear Activation Data, IAEA, Vienna (1987) 83.
[69] GANEEV, A.S., GOVOROV, A.M., OSETINSKII, G.M., RAKIVNENKO, A.N., SIZOV, I.V., SIKSIN, V.S., Sov. J. At. Energy, Suppl. No. 5 (1957) 21.
[70] DAVIDENKO, V.A., KUCHER, A.M., POGREBOV, I.S., TUTUROV, I.F., Sov. J. At. Energy, Suppl. No. 5 (1957) 7.
[71] GOLDBERG, M.D., LeBLANC, J.M., Phys. Rev. **119** (1960) 1992.
[72] THORNTON, S.T., Nucl. Phys., A **136** (1969) 25.
[73] McNEILL, K.G., Philos. Mag. **46** (1955) 800.
[74] HALE, G.M., Muon Catal. Fusion **5** (1990) 227.
[75] CORE, W.G.F., A Note on the Computation of Thermonuclear Reactivities in Plasma-Fusion Applications, Tech. Rep. JET-IR(87)11, JET Joint Undertaking, Abingdon, Oxfordshire (1987).
[76] FUTCH, A.H., Jr., HOLDREN, J.P., KILLEEN, J., MIRIN, A.A., Plasma Phys. **14** (1972) 211.
[77] NIIKURA, S., NAGAMI, M., Fusion Eng. Des. **12** (1990) 467.
[78] TUCK, J.L., Thermonuclear Reaction Rates, Tech. Rep. LAMS-1640, Los Alamos National Laboratory, Los Alamos, NM (1954).
[79] TUCK, J.L., Nucl. Fusion **1** (1961) 201.
[80] GREENE, S.L., Jr., Maxwell Averaged Cross Sections for some Thermonuclear Reactions on Light Isotopes, Tech. Rep. UCRL-70522, Lawrence Radiation Laboratory, Livermore, CA (1967).
[81] JARMIE, N., SEAGRAVE, J.D., ALLEN, R.C., et al., Charged Particle Cross Sections, Tech. Rep. LA-2014, Los Alamos Scientific Laboratory, Los Alamos, NM (1956).
[82] McNALLY, J.R., Jr., ROTHE, K.E., SHARP, R.D., Fusion Reactivity Graphs and Tables for Charged Particle Reactions, Tech. Rep. ORNL/TM-6914, Oak Ridge National Laboratory, Oak Ridge, TN (1979).
[83] BRUNELLI, B., Nuovo Cim., B **55** (1980) 264.
[84] BRUECKNER, K.A., JORNA, S., Rev. Mod. Phys. **46** (1974) 325.
[85] JOHNER, J., Optimized Monomial Approximations with Integer Exponents of the Deuterium-Tritium Thermonuclear Reaction Rate, Tech. Rep. EUR-CEA-FC-1320, Centre

d'études nucléaires de Cadarache, Saint-Paul-lez-Durance (1987).
[86] SLAUGHTER, D., J. Appl. Phys. **54** (1983) 1209.
[87] MILEY, G.H., TOWNER, H., IVICH, N., Fusion Cross Sections and Reactivities, Tech. Rep. COO-2218-17, Univ. of Illinois, Urbana, IL (1974).
[88] SADLER, G., JARVIS, O.N., Van BELLE, P., HAWKES, N., SYME, B., in Controlled Fusion and Plasma Physics (Proc. 14th Eur. Conf. Madrid, 1987), Vol. 11D, Part III, European Physical Society (1987) 1232.
[89] BATISTONI, P., BARNES, C.W., Plasma Phys. Control. Fusion **33** (1991) 1735.
[90] LEINBERGER, U., Untersuchung der Fusions-Protonen- und Tritonenemission an ASDEX, Tech. Rep. IPP-III/171, Max-Planck-Institut für Plasmaphysik, Garching (1990).
[91] HALE, G.M., SMITH, R.D., TALLEY, T.L., J. Fusion Energy **9** (1990) 187.
[92] BALIN, D.V., MAEV, E.M., MEDVEDEV, V.L., et al., Phys. Lett., B **141** (1984) 173.
[93] BALIN, D.V., VOROB'EV, A.A., VOROB'EV, A.A., et al., JETP Lett. **40** (1984) 1112.
[94] WHITE, R.M., RESLER, D.A., WARSHAW, S.I., in Nuclear Data for Science and Technology (Proc. Int. Conf. Jülich, 1991), Springer-Verlag, Berlin (1991) 834.
[95] ABRAMOVICH, S.N., GUZHOVSKIJ, B.Ya., ZHEREBTSOV, V.A., ZVENIG-ORODSKIJ, A.G., Nuclear Physics Constants for Thermonuclear Fusion — A Reference Handbook (in Russian); English Translation: IAEA Rep. INDC(CCP)-326/L+F, IAEA, Vienna (1991).

(Manuscript received 30 September 1991
Final manuscript received 21 January 1992)